

Analysis and Suppression of Common Mode Interference in Three-Phase Power Rectifier Unit Based on Common Mode Transformer

JINFENG LIU¹, YU ZHANG¹, XUDONG WANG¹, and RUI GONG²

¹School of Electrical & Electronic Engineering, Harbin University of Science & Technology, CHINA

²State Grid Heilongjiang Electric Power Company Limited, CHINA

ljf78118@163.com, 494265514@qq.com, wxd6158@163.com, blackdoor629@163.com

Abstract: - Power rectifier unit can realize converting current by use of three-phase synchronous rectification bridge. The multiple parallel power units can amplify the capability of single generator and it is invaluable in battery charge, welding machine and electrochemistry fields. Nevertheless, the electromagnetic interference (EMI) which results from the speedy switch of power devices would affect the parallel output voltage, even out of control. According to the structure of power rectifier unit in this paper, the current path and magnitude of common mode (CM) conducted interference which ranges from 10kHz to 30MHz would be more analysed. The simulation model with parasitic parameters based on SPWM control model was built in this paper and then contrasted the different suppression methods by use of inductor and transformer respectively. At last, the line impedance stability network (LISN) and EMI receiver were used to test the common mode interference (CMI) of power rectifier unit. The experiment result verified the accuracy of model and validity of suppression method with CM transformer.

Key-Words: - Electromagnetic Interference, Common Mode Transformer, Conducted Interference, Power Rectifier Unit, Line Impedance Stability Network.

1 Introduction

The traditional apparatus with high direct current consists of multiple parallel DC power modules in order to output high current and they share the high power output. With the improvement of request for production process and efficiency in many companies, the deficiencies of this kind of power become more and more. First of all, it has high energy consumption and low efficiency. Secondly, the whole volume is large and weight is heavy because the power frequency transformer is usually used and many power modules are paralleled. Lastly, the control apparatus has low precision and high energy consumption [1-2]. The low voltage and high direct current power supply based on mature synchronous alternator in this paper has multiple parallel power units. Each unit consists of three-phase windings and three-phase synchronous rectification system. The use of MOSFET can greatly reduce the power converter's volume and weight and better the quality of high frequency power supply. DC power supply can be delivered to DC bus after rectification and the number of parallel power units can be varied to satisfy the power need of different load.

Although every three-phase synchronous rectifier unit with power switch can fast the dynamic response, high frequency pulse which is produced by switch will lead to high change rate of current and voltage and become strong EMI, where the CMI is dominant [3].

The frequency of this kind of interference ranges from two or three kilohertz to dozens of megahertz and magnitude has exceeded over the electromagnetic compatibility (EMC) limit. EMI of rectifier would influence not only the normal procedure of load but rectifier itself. A mass of retrieval material can prove that strong voltage change rate produced by neutral point of rectifier to ground could charge and discharge the parasitic capacitors, so the CMI of three-phase rectifier unit is primarily due to DC side [4-6]. Analysis and suppression CMI for rectifier unit are so useful that it's crucial to optimize the quality of DC output and improve the EMC performance.

Section 2 presents the common mode current loop of voltage mode PWM rectifier. Section 3 presents the simulation module of separate and entire power unit. Section 4 presents suppress method of common mode EMI. Section 5 presents the experiment results by test platform.

2 Common Mode Current of the Voltage Mode PWM rectifier

The thyristor rectification circuit is usually used to traditional three-phase power supply. It would bring low power factor and a fair amount of resonance to power supply when thyristor's turn-on angle is smaller. So the extra apparatus with the function of eliminating resonance and power factor compensation

is widely applied to large bulk thyristor rectifier, therefore, it will increase the consumer's cost. In this paper each unit with efficient and high frequency power has the voltage mode PWM rectifier whose switches are MOSFETs of extremely low on-resistance. It can convert AC to DC and realize stable DC output. This kind of rectifier would improve energy efficiency, reduce the reactive power and resonance and raise the quality of energy [7-8].

The structure of high frequency power supply based on the voltage mode PWM rectifier is shown in Fig.1. Three-phase PWM rectifier is composed of three half bridges, namely, six MOSFETs. The input side of AC connects to power supply through three-phase inductance which simulates the inner of synchronous alternator.

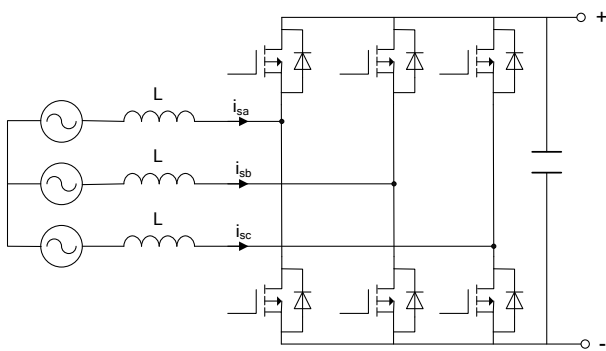


Fig.1 High Frequency Power Structure of PWM Rectifier

Voltage change in the switch circuit of PWM rectifier is so rapid that can reach 10kV/μs and then couples to parasitic capacitors. Consequently, CMI forms on the input and output ports. For the structure reliability, MOSFET heatsink usually screws tightly to the shell of machine which is connected to ground in order to don't electrocute when someone touches shell. Insulation layer between switch and heatsink is very thin, that is, the metal cooling fin of switch adheres to heatsink through grease in case of overheat failure for switch. So parasitic capacitor would be formed between the drain or source of switch and heatsink. CM voltage will charge and discharge parasitic capacitor continuously and produce CM current [9]. Approximately formula of parasitic capacitor:

$$C_p = 8.85 \times 10^{-12} \times \frac{\epsilon_r A}{h} \tag{1}$$

where ϵ_r is the relative permittivity between power switch and heatsink, A is the area of heatsink, h is the thickness of insulated spacer. According to the material of insulator and structure of heatsink, we can get the parameters as below: $\epsilon_r = 2.2$, $A = 3.1\text{cm}^2$, $h = 2\text{mm}$, then $C_p = 30\text{pF}$.

But the parasitic capacitor which is neutral to ground in a leg of PWM rectifier is combining between top and bottom switch. When they both have identical characteristics, the parasitic capacitor in every leg is about double than in single switch.

Because parasitic parameters to ground could influence CMI seriously and the impedance of line itself isn't ideal, we should keep stability of line to ground by connecting LISN to circuit on the basis of standard GBT17626. The previous researches show that differential mode (DM) interference is mainly in AC side of rectifier, while CMI is dominantly produced by DC side [10]. LISN is placed into the DC side in the testing procedure. Since LISN has the characteristics of stable impedance, we can consider LISN impedance to ground as line impedance to ground in the following analysis.

There are two paths of CM current which are shown in Fig.2. Broken line 1 is one of CM current that flows input of rectifier. It flows through heatsink to referenced ground and then flows back through parasitic capacitor of AC power supply [11]. In generally, the parasitic capacitors of AC power supply to ground is much greater than switch to ground and their influence to CM current can be ignored. Broken line 2 is the other of CM current. It flows back through testing LISN.

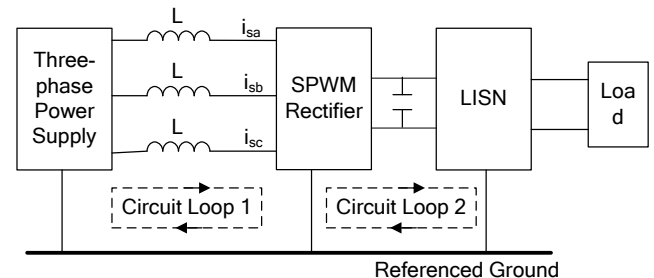


Fig.2 Coupled path of CM Current

Fig.3 shows the result of conducted interference when LISN is inserted between filter capacitor and load. Conducted interference of entire system concentrates on the range from 5MHz to 30MHz which is obviously frequency scope of CMI. This paper will focus on this scope to analyse and reduce the interference.

Maximum interference is on 20MHz, whose value reaches almost 60dB, and the damping rate is about 30dB/dec. CM filter could provide damping of 40dB/dec in perfect circumstance, that is, the impedance of CM noise source and load are ignored [12]. Filter must provide damping of 30dB/dec at least when impedance of noise source and load are considered, and then it can satisfy the design demand.

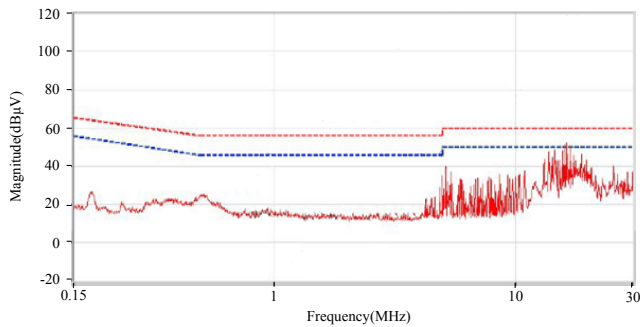


Fig.3 CMI result of rectifier

3 Simulation Model of Power Rectifier Unit

There are passive devices such as resistor, capacitor etc. on the output of rectifier unit. They generally regard as pure resistor or capacitor in the design process, while they all have separately parasitic parameters within the high frequency, especially the radio frequency whose range from 1MHz to 30MHz. They dramatically affect EMC of device [13]. The high frequency characteristics of these passive devices must be considered when we analyse CMI.

3.1 High Frequency Characteristic of Resistor

The resistor's impedance characteristic is different from ideal since it is typical load for rectifier. Fig.4 is high frequency equivalent circuit of resistor, where L_r is leakage inductance and C_r is parasitic capacitor of resistor.

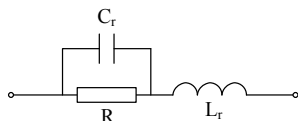


Fig.4 High frequency equivalent circuit of resistor

For large resistor, parasitic capacitor is dominant within high frequency. Nevertheless, for small resistor, main parasitic parameter is inductor. Fig.5 and Fig.6 are impedance characteristics which range from 10kHz to 30MHz for 500kΩ and 100mΩ, respectively. It's evident that 500kΩ resistor still keep resistance within 1MHz, and magnitude falls at the rate of -20dB/dec over 1MHz which is the state of capacitance, meanwhile, the phase reaches -90° .

For 100mΩ resistor, parasitic inductor is effective and magnitude arises at the rate of 20dB/dec within the whole testing frequency. The phase reaches 90° . Applied load in this system is winding resistor with low resistance and parasitic inductor is principal in high frequency. We can get the parameters of resistor

through impedance analyser and Saber simulation fitting curve as below: $R=100m\Omega$, $L_r=80nH$, $C_r=0$.

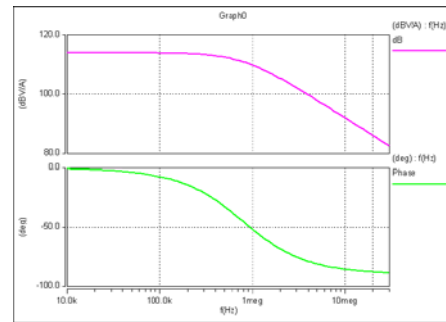


Fig.5 Impedance characteristics of 500kΩ resistor

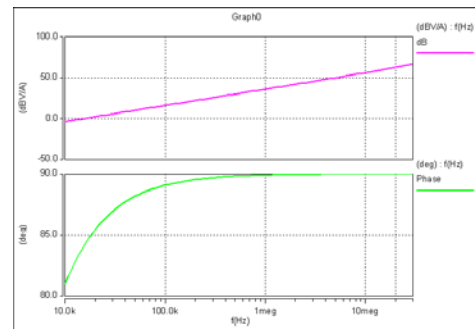


Fig.6 Impedance characteristics of 100mΩ resistor

3.2 High Frequency Characteristic of Capacitor

Real capacitor exists stray inductors and high frequency equivalent circuit is shown in Fig.7, where L_c is leakage inductor, R_c is equivalent series resistor. The equivalent parameters of 4700μF electrolytic capacitor in this system are listed as below: $L_c=10nH$, $R_c=30m\Omega$.

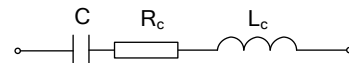


Fig.7 High frequency equivalent circuit of capacitor

Fig.8 represents the impedance characteristic of this capacitor. The impedance of capacitor is so high that can regard as open in the circumstance of DC and low frequency. Capacitor C would play main role if frequency was high and magnitude falls at the rate of -20dB/dec.

Corner frequency emerges when impedance of capacitor and stray inductor are almost equal. Therefore, magnitude arises at the rate of 20dB/dec and phase swiftly reaches 90° because stray inductor prevails during this period.

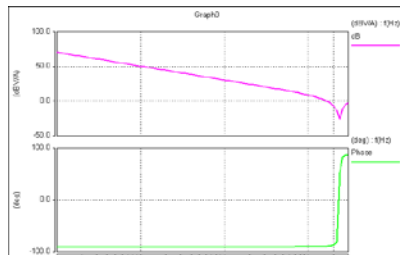


Fig.8 Impedance characteristics of 4700uF capacitor

3.3 Simulation Model of Entire Power Rectifier Unit

The simulation model for power rectifier unit can be built according to aforementioned parameters which is shown in Fig.9. C_p is parasitic capacitor of every rectifier leg's neutral to ground which is a composite of up and bottom switches, whose value is almost twice of equation (1). LISN introduces $0.25\mu\text{F}$

capacitor and 50Ω resistor for each line of DC output to ground. C_n is the parasitic capacitor of DC line to ground. Meanwhile, the model considers the parasitic parameters of filter capacitor and load.

In order to achieve high efficiency and fast response, the method of load power feedforward without different beat is applied to this paper. This method can not only improve the performance of dynamic response for PWM rectifier but also trace the variance of load power real-timely through the test of load power and feedforward compensation. Meanwhile, it can fast trace current signal of DC bus without difference and reduce the distortion of voltage and current of power supply through the PWM rectification technology with high power factor. The fundamental idea of this method is to calculate the pulse width of next switch period according to the state equation of DC system, feedback signal and required next referenced output value.

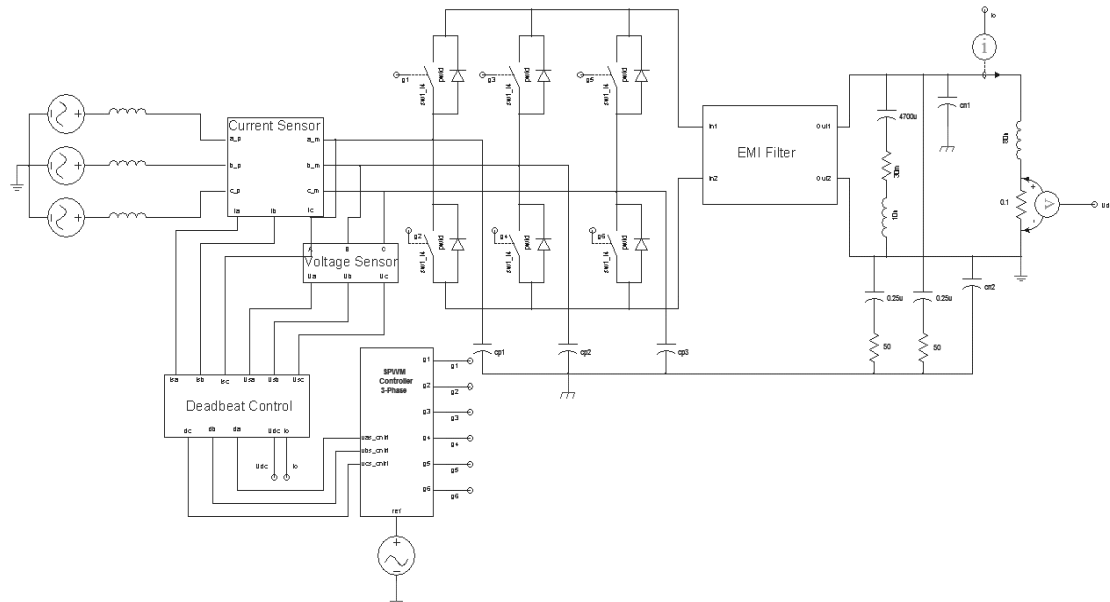


Fig.9 Simulation model with parasitic parameters of power rectifier unit

The MOSFET is FDP8030L which is product of Fairchild Semiconductor Incorporation. According to the parameters of this MOSFET, we set about the model of switch as below: turn-on rise time $t_r=185\text{ns}$, turn-off fall time $t_f=200\text{ns}$, on-state resistance $r_{on}=3.5\text{m}\Omega$.

Fig.10 is converting scheme of single rectifier leg. CM current flows through parasitic capacitor C_p and heatsink to referenced ground, and then flows back to DC side through $0.25\mu\text{F}$ capacitor and 50Ω resistor of LISN. It divides into two paths, i.e. current I_1 and I_2 , where I_1 flows back positive DC line directly and I_2 flows back through electrolytic capacitor and load. For convenience, the parasitic capacitors of DC line to

ground can be ignored since they connect LISN in parallel completely [14].

Although there are equivalent series inductor and resistor for electrolytic capacitor, its inductor is much less than the parasitic inductor of CM loop circuit and its resistor is much lower than 50Ω of LISN. Consequently, parasitic inductor and resistor of electrolytic capacitor can be ignored, while capacitance of series-connected $4700\mu\text{F}$ and $0.25\mu\text{F}$ is almost $0.25\mu\text{F}$. Otherwise, the resistance of load is very low because we want to produce low voltage and high current DC output. So the paths of current I_1 and I_2 are nearly same.

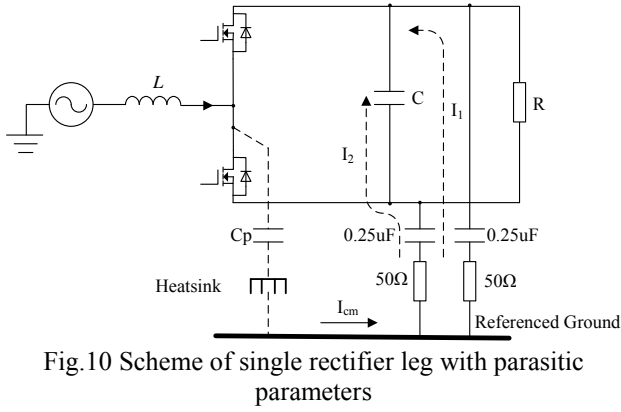


Fig.10 Scheme of single rectifier leg with parasitic parameters

Fig.11 is equivalent circuit of CMI for three legs. V_1, V_2 and V_3 are interferential source of every leg's neutral. R_o is a composite of resistor of DC line and load. L_{cm} is equivalent inductor between heatsink and referenced ground and L_{sn} is equivalent inductor between LISN and electrolytic capacitor. Fig.11(b) shows that simplified equivalent circuit, where L is the sum of $L_{sn}/2$ and L_{cm} , R is almost 25Ω because R_o is much lower than 25Ω . Otherwise, $0.5\mu F$ capacitor can be ignored because either C_p or C_n is much less than $0.5\mu F$ and the series result is nearly equal to the sum of C_p and C_n . We can get the circuit parameters by impedance analyser and corresponding calculation as below: $L_{sn}=8\mu H, L_{cm}=2\mu H, C_n=1200pF, C_p=60pF$. Consequently, the last CM equivalent circuit is second-order RLC circuit, where $L=6\mu H, R=25\Omega, C=1260pF$.

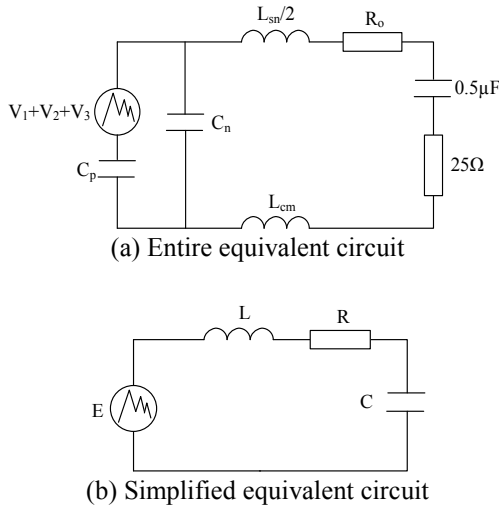


Fig.11 Equivalent circuit of CMI

According to RLC circuit, CM current, i.e. resonant current is:

$$i(t) = \frac{E}{\sqrt{1-\xi^2}Z_0} e^{-\xi\omega_n t} \sin(\sqrt{1-\xi^2}\omega_n t) \quad (2)$$

where $\omega_n = \frac{1}{\sqrt{LC}}$, $\xi = \frac{R}{2}\sqrt{\frac{C}{L}}$, $Z_0 = \sqrt{\frac{L}{C}}$. They represent resonant angular frequency, damping coefficient and characteristic impedance, respectively.

4 Suppress of Common mode EMI for Power Rectifier Unit

Usual method to suppress common mode interference is EMI filter. CM capacitor can reduce CM interferential source, while CM inductor can increase impedance of loop circuit which would reduce CM current [15]. This paper consults the method of CM transformer which could attenuate axial current and then proposes the CM transformer which is put in DC side to suppress CMI.

4.1 Analysis of CM Inductor used in DC Side

CM inductor is essentially transformer whose turns ratio is 1:1, while the methodology of connecting is different. Fig.12 is the symbol and structure of CM inductor and Fig.12(b) demonstrates the direction of windings and magnetic field. Flux H_{CM} will superpose upon each other and inductance could increase when CM current flows through CM inductor. Nevertheless, flux H_{DM} will offset by each other and inductance is almost zero when DM current flows through CM inductor. Namely, CM inductor performs high impedance for CM current and low impedance for DM current. So it can mainly reduce CMI. CM inductor is useful to suppress CMI of low frequency, while larger CM inductor would reduce less CMI of high frequency since the increase of winding turns results in the increase of distributed capacitor.

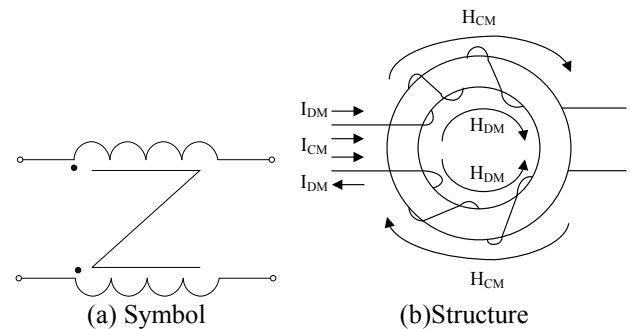


Fig.12 Common mode inductor

CM inductor is placed between DC output and LISN which is shown in Fig.13. CM inductor can be equivalent to inductor and resistor in series if CM inductor's parasitic capacitor was ignored.

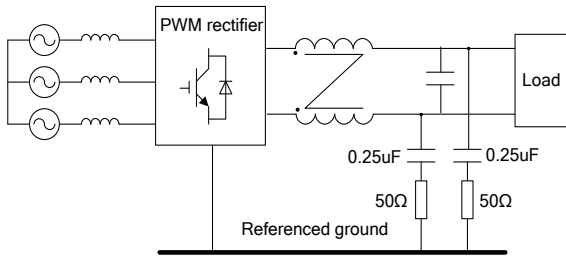


Fig.13

Test scheme with common mode inductor

Suppose the L and R of series resonant circuit are n times and m times respectively than original and then the characteristic parameters are:

$$\omega'_n = \frac{1}{\sqrt{nLC}} = \frac{1}{\sqrt{n}} \omega_n \quad (3)$$

$$\xi' = \frac{mR}{2} \sqrt{\frac{C}{nL}} = \frac{m}{\sqrt{n}} \xi \quad (4)$$

$$Z'_0 = \sqrt{\frac{nL}{C}} = \sqrt{n} Z_0 \quad (5)$$

So CM current is updated as:

$$i(t) = \frac{E}{\sqrt{n - (m\xi)^2} Z_0} e^{-m\xi\omega_n t/n} \sin(\sqrt{n - (m\xi)^2} \frac{\omega_n}{n} t) \quad (6)$$

Since $n \gg (m\xi)^2$ in CM inductor, resonant current can be simplified as:

$$i(t) = \frac{E}{\sqrt{n} Z_0} e^{-m\xi\omega_n t/n} \sin(\frac{\omega_n}{\sqrt{n}} t) \quad (7)$$

Ferrite core of CM inductor is EE16 with 8 winding turns for each. Cross-sectional area of magnetic ring is 0.19cm^2 and length of it is 1.7cm . Each inductance is 0.735mH by calculation. Coupled equivalent inductor is 0.75mH which is tested by impedance analyser, that is, the leakage inductance of each winding is $3\mu\text{H}$.

The structure of CM inductor is similar to ring transformer because they both are composed of magnetic ring and two windings. Coupled inductor in Saber can simulate CM inductor and designate P ports of each coupled inductors as dotted terminal. Connected inductor and coupled inductor are set 0.753mH and 0.75mH respectively. Fig.14 is the simulation model of coupled inductor.

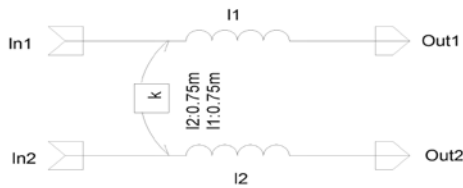


Fig.14 Model of coupled inductor

Frequency spectrum of CM loop impedance with CM inductor is shown in Fig.15. Fig.16 presents frequency spectrum of CM current by AC small signal analysis of Saber. According to the simulation result,

CM inductor can provide higher impedance from 10kHz to 2MHz and lower impedance over corner frequency. So CM inductor has limit ability to reduce CMI of high frequency.

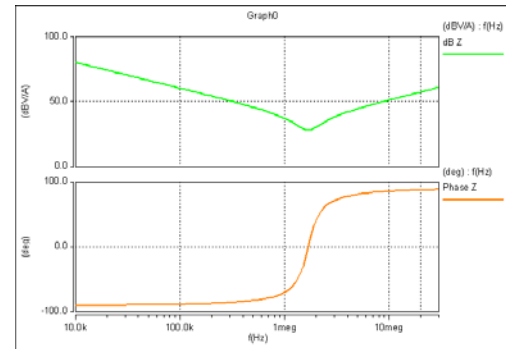


Fig.15 Impedance analysis of CMI loop circuit

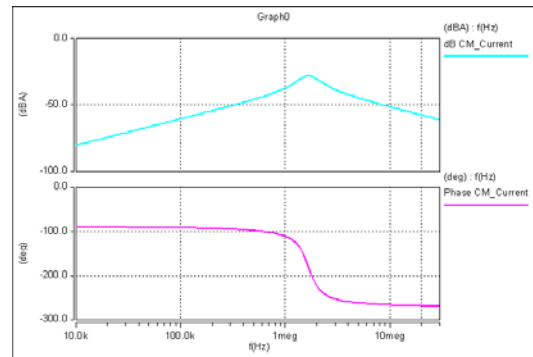


Fig.16 Frequency spectrum of CM current

4.2 Analysis of CM Transformer used in DC Side

CM transformer can form by adding secondary winding L_m based on CM inductor. R_i is in parallel with secondary winding. L_m could induce current when flux is variable in CM transformer caused by CM current but DM current would offset. Fig.17 represents the structure of CM transformer with six ports.

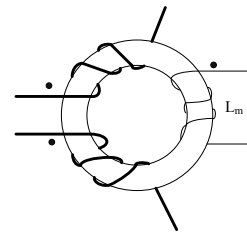


Fig.17 Structure of CM transformer

Two primary windings turns are still 8 and new secondary winding turns is also 8. Secondary winding is thin in order to attenuate core window area since the secondary current is very low and parallel resistor can be chose on the basis of suppression request. Fig.18

demonstrates the test scheme when CM transformer is placed on DC side of rectifier.

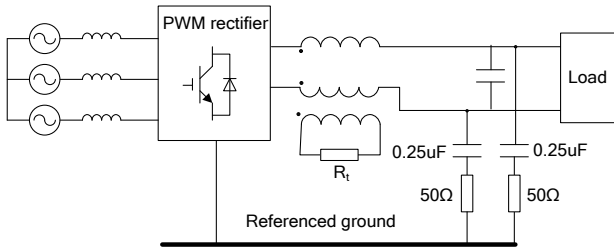


Fig.18 Test scheme with CM transformer

The transfer function of CM equivalent circuit should be analysed and then determine the resistance of R_t . Fig.19 is equivalent circuit with CM transformer which is replaced with T type circuit. L_1 , L_2 and L_m are leakage inductance of two primary windings and inductance of exciting winding respectively. We can get parameters after testing as below: $L_m=0.6mH$, $L_1=L_2=3\mu H$.

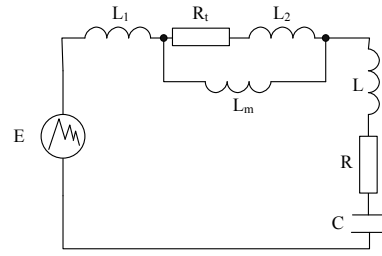


Fig.19 Equivalent circuit with CM transformer

According to equivalent circuit of Fig.17, the transformer function of CM current to voltage source is:

$$\frac{I_{cm}(s)}{E(s)} = \frac{1}{L_1s + L_ms // (R_t + L_2s) + Ls + R + 1/Cs} \quad (8)$$

where L_1 combines with L to form L_t for convenience and the function after sorting out is:

$$\frac{I_{cm}(s)}{E(s)} = \frac{sC[s(L_2 + L_m) + R_t]}{s^3C(LL_2 + LL_m + L_mL_2) + s^2C[R(L_2 + L_m) + R_t(L_2 + L_m)] + s(L_2 + L_m + RR_tC) + R_t} \quad (9)$$

Since $L_2 \ll L_m$, $L_t \ll L_m$, $RR_tC \ll L_m$, the characteristic equation is:

$$s^3CL_m(L + L_2) + s^2CL_m(R + R_t) + sL_m + R_t = 0 \quad (10)$$

Based on a analysis of Matlab root locus, there are two conjugate complex roots and a real root when $0 < R_t < 120\Omega$. CM current determined by two complex roots is oscillating because the real root is offset by zero on the origin. There are three real roots when $120\Omega < R_t < 350\Omega$. CM current is determined by next pole to the origin because the pole which is closest to the origin is offset by zero and its wave is damping exponentially.

There are two complex roots and a real root when $R_t > 350\Omega$. CM current is determined by two complex roots since the real root is far away from the origin and its wave is still oscillating.

Fig.20(a)-(c) represent zeros-poles distribution for CM current loop circuit when R_t is 2Ω , 200Ω and 1000Ω , respectively. The result is in accordance with aforementioned analysis. Especially, two complex roots are on the vertical axis and system is critically stable state when $R_t=1000\Omega$.

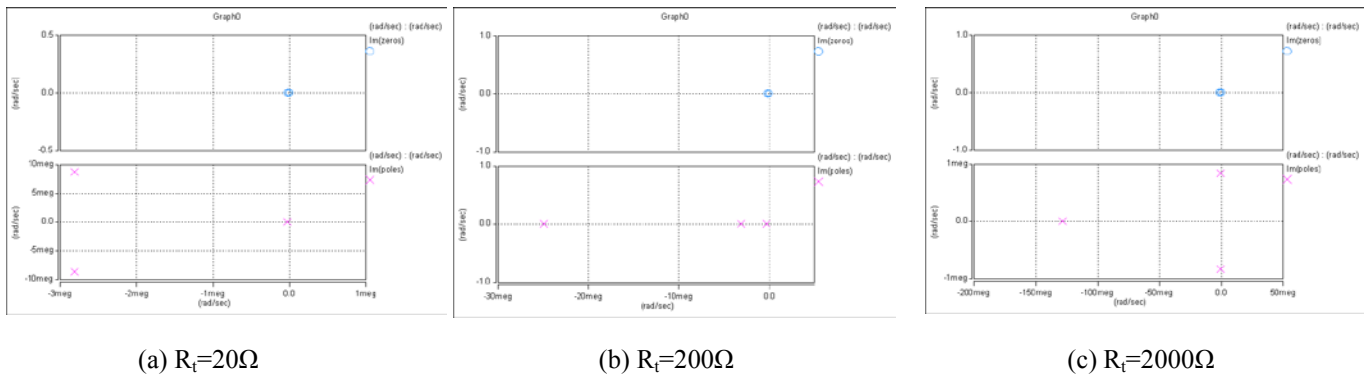


Fig.20 Poles-Zeros distribution

The choice of R_t can make three real roots for characteristic equation and CM current can not

oscillate. Eventually, R_t is 200Ω and CM current is determined by next pole to the origin. Fig.21 is CM

transformer model in Saber where exciting winding is in parallel with R_t .

Frequency spectrum of CM loop impedance with CM transformer is shown in Fig.22. Fig.23 represents frequency spectrum of CM current by AC small signal analysis of Saber. According to the simulation result, CM transformer provides low impedance from 10kHz to 200kHz, while high impedance after corner frequency. Especially, impedances are all higher than them at the range of low frequency over 1MHz. So it's efficient for suppression of high frequency CMI.

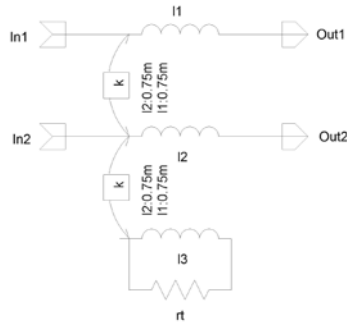


Fig.21 Saber model of coupled transformer

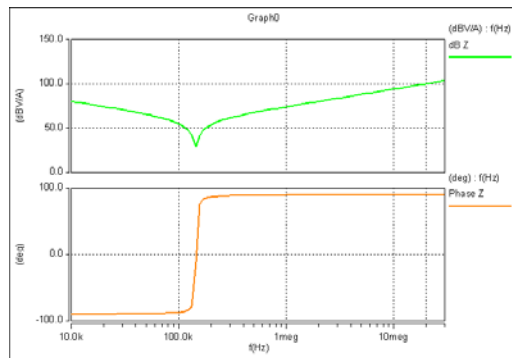


Fig.22 Impedance analysis of CMI loop circuit

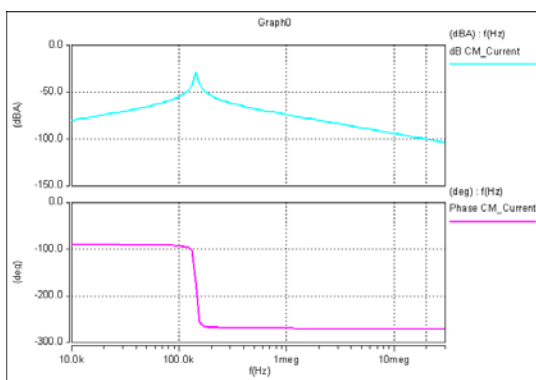


Fig.23 Frequency spectrum of CM current

5 Experiment of Validation

In order to verify the model and EMI suppression method, CMI testing platform for power rectifier unit is built. AFJ instruments is used to test CM conducted interference which is shown in Fig.24.

Fig.25 represents CMI spectrum through EMI receiver and LISN when CM inductor was applied to system. It's obvious that CM inductor can attenuate CMI on the range of low frequency but can not reduce CMI on high frequency which is important area to control. On the other hand, CMI on high frequency is higher because partial of DMI converts to CMI based on the existence of CM inductor.



Fig.24 Test system of CM conducted interference

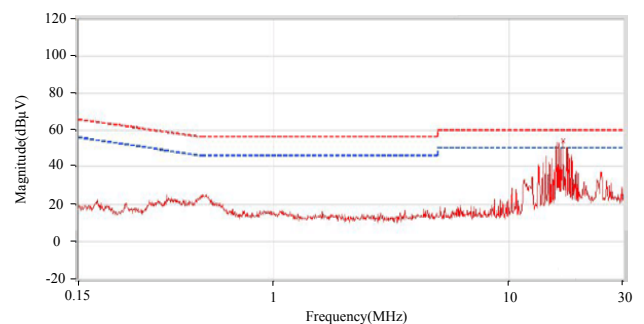


Fig.25 CMI spectrum with CM inductor

Fig.26 and 27 show CMI spectrum when parallel resistor R_t in CM transformer is 100Ω and 200Ω, respectively. CMI is attenuated effectively on the range of high frequency because of the existence of parallel resistor. The characteristic equation has two complex roots and a real root when $R_t=100\Omega$. Therefore, although CM current is reduced, it oscillates. The characteristic equation has three real roots when $R_t=200\Omega$. CM current is attenuated on the entire range of testing frequency. It can prove the accuracy of model and validity of suppression method.

6 Conclusion

This paper analyzed coupled path of CM current of SPWM rectifier and deduced CMI was produced by charging and discharging for parasitic capacitor of leg's neutral to ground. RLC resonant equivalent circuit was built to simulate CM current loop. The principle and suppression result for CMI were

compared when CM inductor and transformer are used respectively. The experiment spectrum result verified accuracy of model and validity of suppression method. While, there are three demerits about CM transformer. First, the structure of CM transformer is more complicate than inductor. Secondly, secondary winding will produce transformer's CM noise through electric field coupling once noise voltage distributes on primary winding. Lastly, the wave ripple of DC output voltage is more high because of the introduction of CM transformer.

Therefore, in order to conquer the defects as stated above, more exact parameters design for CM transformer must be done in the future according to the characteristics of transformer.

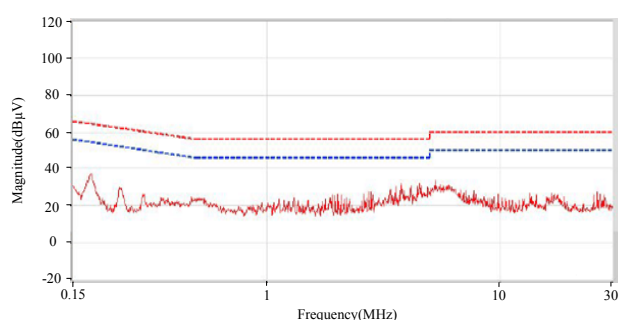


Fig.26 CMI spectrum with CM transformer when $R_t=100$

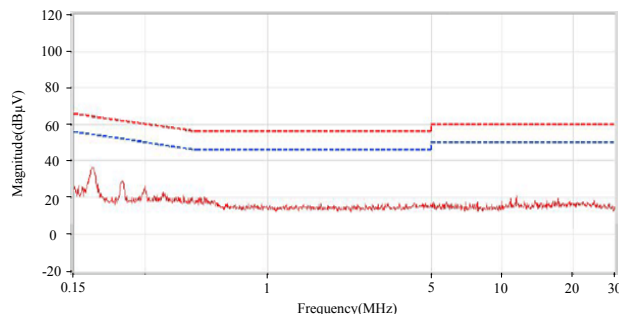


Fig.27 CMI spectrum with CM transformer when $R_t=200$

Acknowledgements

This research was supported by the National Natural Science Foundation of China (No. 51177031) and Key Technology Research of Heilongjiang(No.GA13A202)

References:

- [1] P. A. Dahono, M. Firmansyah, D. Pramasti Y., A high-current low-voltage DC power supply, *IEEE Power Electronics and Drive Systems*, Denpasar, Indonesia, 2001.
- [2] Qamaruzzaman, A. Purwadi, P.A. Dahono, A DC high-current low-voltage power generating system, *IEEE Power System Technology Conference*, Kunming, China, 2002.
- [3] MH Hedayati, AB Acharya, Common-mode

filter design for PWM rectifier-based motor drives, *IEEE Transactions on Power Electronics*, Vol.28, No.11, 2013, pp.5364-5371.

- [4] Pei Xue-jun, Zhang Kai, Kang Yong, Chen Jian, Damping and Suppression of common mode interference currents in PWM inverter, *Proceedings of the CSEE*, Vol.24, No.11, 2004, pp.80-84.
- [5] Lei Xing, Jian Sun, Wai Rongjiong, Conducted common-mode EMI reduction by impedance balancing, *IEEE Transaction on Power Electronics*, Vol.27, No.3, 2012, pp.1084-1089.
- [6] Z. Zhan, Y. Zhong, H. Gao, L. Yuan, Hybrid selection harmonic elimination PWM for common-mode voltage reduction in three-level neutral-point-clamped inverters for variable speed induction drives, *IEEE Transactions on Power Electronics*, Vol.27, No.3, 2012, pp.1152-1158.
- [7] Johann W. Kolar, Thomas Friedli, Jose Rodriguez, Patrick W. Wheeler, Review of three-phase PWM AC-AC converter topologies, *IEEE Trans. Ind. Electron.*, Vol.58, No.11, 2011, pp.4988-5006.
- [8] Fonseca Davide, Cabrita Carlos, Calado Maria, Some design aspects concerning a new single-phase AC/DC PWM converter for ac traction systems, *WSEAS Trans. Circuits Syst.*, Vol.4, No.9, 2005, pp.1019-1027.
- [9] Tokuda Masamitsu, Ohsaki Hiruyuki, Mastuo Takashi, Conducted interference immunity characteristics to high-speed power line communication system, *IEEE International Symposium on Power Line Communications and Its Applications*, Udine, Italy, 2011.
- [10] He Hong, Bao Shuai, Li Hang, Suppression of the conducted interference of switching power supply, *Key Engineering Materials*, Vol.474, No.2, 2011, pp.883-887.
- [11] Sun Ya-xiu, Sun Rui-feng, Chen Bing-cai, Forecast of conducted interference of three-phase PWM drive motor system, *Electric Machines and Control*, Vol.15, No.5, 2011, pp.42-48.
- [12] Darie E., Cepisca C., About the high-frequency interferences produced in systems including PWM and AC motors, *Proceedings of the 12th WSEAS International Conference on Circuits*, Heraklion, Greece, 2008.
- [13] Fucun Han, Shanhong He, Denren Feng, Binying Peng, The conducted interference of electromagnetic pulse toward switch trigger system, *IEEE Conference on Industrial Electronics and Applications*, Hangzhou, China,

2014.

- [14] ML Heldwein, T Nussbaumer, JW Kolar, Common mode modelling and filter design for a three-phase buck-type pulse width modulated rectifier system, *IET Power Electronics*, Vol.3, No.2, 2010, pp.209-218.
- [15] JW Shin, H Shin, GS Seo, JI Ha, Low-common mode voltage H-bridge converter with additional switch legs, *IEEE Transactions on Power Electronics*, Vol.28, No.4, 2013, pp.1773-1782.